doi:10.1016/j.jmb.2007.10.027 J. Mol. Biol. (2008) 375, 331–336

JMB

Available online at www.sciencedirect.com

ScienceDirect

ELSEVIER

COMMUNICATION

Crystallographic Conformers of Actin in a Biologically Active Bundle of Filaments

Yao Cong[1]*, Maya Topf[2], Andrej Sali[2], Paul Matsudaira[3], Matthew Dougherty[1], Wah Chiu[1] and Michael F. Schmid[1]

[1]*National Center for Macromolecular Imaging and Verna and Marrs McLean Department of Biochemistry and Molecular Biology, Baylor College of Medicine, Houston, TX 77030, USA*

[2]*Department of Biopharmaceutical Sciences, University of California at San Francisco, San Francisco, CA 94158, USA*

[3]*Whitehead Institute and Department of Biology and Division of Biological Engineering, Massachusetts Institute of Technology, Cambridge, MA 02142, USA*

Received 12 August 2007; received in revised form 8 October 2007; accepted 9 October 2007
Available online 16 October 2007

Edited by M. Moody

Actin carries out many of its cellular functions through its filamentous form; thus, understanding the detailed structure of actin filaments is an essential step in achieving a mechanistic understanding of actin function. The acrosomal bundle in the *Limulus* sperm has been shown to be a quasi-crystalline array with an asymmetric unit composed of a filament with 14 actin–scruin pairs. The bundle in its true discharge state penetrates the jelly coat of the egg. Our previous electron crystallographic reconstruction demonstrated that the actin filament cross-linked by scruin in this acrosomal bundle state deviates significantly from a perfect F-actin helix. In that study, the tertiary structure of each of the 14 actin protomers in the asymmetric unit of the bundle filament was assumed to be constant. In the current study, an actin filament atomic model in the acrosomal bundle has been refined by combining rigid-body docking with multiple actin crystal structures from the Protein Data Bank and constrained energy minimization. Our observation demonstrates that actin protomers adopt different tertiary conformations when they form an actin filament in the bundle. The scruin and bundle packing forces appear to influence the tertiary and quaternary conformations of actin in the filament of this biologically active bundle.

Keywords: actin; electron cryomicroscopy; acrosomal bundle; energy minimization; conformational heterogeneity

During the *Limulus* acrosomal reaction, a bundle of actin filaments cross-linked by scruin uncoils and supports an extension of the plasma membrane that mechanically penetrates through the jelly layer surrounding the egg membrane.[1] Biomechanical studies show that the extended bundle has a Young's modulus in the giga-Pascal range.[2] The coiled bundle stores approximately 10^{-13} J of elastic energy.[2]

The extended form of the bundle, which is also known as the true discharge state, is a three-dimensional crystal obeying the symmetry of space group $P2_1$ with 14 actin and scruin protomers in the asymmetric unit.[3] The 9.5-Å cryo-electron microscopy (cryoEM) map of the bundle[4] showed that its actin filament is not strictly helical as in the Holmes F-actin filament model.[5] A single model for an individual F-actin protomer (courtesy of K. Holmes) was fitted as a rigid body into each of the 14 actin positions in the filament in our cryoEM density map. We will refer to this model as the homogeneous starting model. The average deviation between the orientation of our model and that of the Holmes F-actin model[5] is 11.3°.[4] The orientation deviations resulted in severe steric clashes between subunits in the homogeneous starting filament model. No refinement was carried out to relieve such clashes in our previous study.[4]

*Corresponding author. E-mail address: mschmid@bcm.tmc.edu.

Abbreviation used: cryoEM, cryo-electron microscopy.

Each actin subunit has four subdomains (Fig. 1a);[6] subdomains 2 and 4 of one molecule interact with subdomains 1 and 3 of the molecule above it in the same strand. The most severe steric clashes in the homogeneous starting model occur at these contacts (Supplemental Movie 1). Other clashes occur between the hydrophobic plug[5] of one subunit and the subunits in the opposite strand. This is because the fit of the plug to the opposite strand is quite snug, and only a slight deviation from the canonical F-actin structure[5] will cause a steric clash. To resolve all these clashes, we carried out energy minimization on this starting model using X-PLOR[7] in combination with Situs[8] to constrain the orientations that were determined above with respect to our cryoEM density fit (Supplemental Materials and Methods). Figure 1b illustrates the refined model based on the Holmes coordinates after minimization. Red highlights the largest movements required by the energy minimization, involving residues for which the C_α needed to be moved by more than 2.5 Å during the minimization. The total number of such residues for this model is 103.

In addition to the Holmes actin filament model, there exist a wealth of monomeric actin (G-actin) crystal structures that vary in their states of the bound nucleotide, crystallization buffers, co-crystallized proteins, and species of origin. These structures share a similar four-subdomain organization but differ in details (Fig. 1a). The spatial relationship of the subdomains in actin is characterized by twist-and-scissors angle differences with respect to the original Holmes crystal structure (Supplemental Movie 2 and Fig. 1a), but the deposited crystal structures, varied as they are, may still not express the entire range of possible conformations available to actin.[9] Based on these differences, we grouped actin structures into four classes: open and closed conformation between subdomains 1 plus 2 and subdomains 3 plus 4 (Fig. 1a)[10]; in the closed conformation group, they can be further subdivided into twisted right (of subdomains 3 and 4, as viewed from the left side of Fig. 1a), twisted left, and untwisted with respect to the original Holmes structure (Supplemental Movie 2). Also, as illustrated in Fig. 1a, the backbone secondary structure of the same residues in subdomain 2 of some actin crystal structures is α-helical (e.g., residues 40–47 in 1J6Z), that in others is β-sheet (e.g., residues 42–44 in 1ATN), and that in yet others is random coil (e.g., residues 38–51 in 2BTF and 1HLU as well as residues 39–55 in 1YAG), or even disordered and unobserved.

To investigate whether the other actin crystal coordinates might provide more suitable models for the actin protomers in the asymmetric unit of the acrosomal bundle in our 9.5-Å cryoEM map,[4] we replaced Holmes coordinates with each of these other actin coordinates at each of the 14 actin positions in the asymmetric unit. These other coordinates were directly superimposed onto subdomain 1 of the Holmes coordinates, which corresponds to the highest density in the averaged cryoEM map. The trial model was accepted if it had minimum clashes with the subunit located above it in the same strand. The identity of the upper subunit in testing these alternatives was of secondary importance, because subdomains 1 and 3 of most actin molecules are quite similar to each other (Fig. 1a); subdomains 2 and 4 of the lower subunit are most critical to (i) the differences in structure, (ii) the causes of steric clashes with the molecule above it in the filament, and (iii) the means of relieving these clashes by choosing a different model. Given the resolution of our cryoEM map (9.5 Å), several actin structures from the same class (see above) fit the map equally well, and thus any of them is equally acceptable; thus, the reliability of a particular model in a particular position in the filament is limited to the class to which it belongs.

Using nine actin coordinate sets for the 14 actin positions in the asymmetric unit (Fig. 1c) resulted in significantly fewer steric clashes between neighboring subunits. We will refer to this model as the heterogeneous starting model. The improvements include fewer clashes between the neighboring subunits in the same strand and between the hydrophobic plug of one subunit and the adjacent subunit in the opposite strand. These hydrophobic plug clashes were generally alleviated because the corresponding loops in these crystal structures do not protrude as far from the surface. There are still some remaining clashes between neighboring subunits belonging to the same strand (notably subunits 4 and 6 as well as subunits 12 and 14) as well as between adjacent subunits in different strands (subunits 9 and 10). To resolve these clashes, we carried out the same energy minimization procedure as described above for the homogeneous starting model. Figure 1d shows our atomic model based on the heterogeneous starting model after energy minimization. The total number of residues with C_α movement larger than 2.5 Å after minimization for this heterogeneous starting model is 29, much fewer than that for the homogeneous starting model (103 residues).

Figure 1b and d demonstrate visually that fewer residues need to be moved by a large distance for the heterogeneous *versus* the homogeneous starting model. In Fig. 2, we show this quantitatively in histogram distributions of C_α atoms' movement during energy minimization for both sets of models. Figure 2 illustrates that the movement of C_α atoms in the heterogeneous starting model has a smaller and tighter distribution compared with the homogeneous starting model. The average C_α movement in the heterogeneous starting model is 0.66 Å, whereas that for the homogeneous starting model is 0.87 Å.

Our acrosomal actin filament model-building process, including rigid-body docking and model refinement by constrained energy minimization, clearly demonstrates that the heterogeneous model is a more appropriate actin filament model because it produces fewer clashes and smaller shifts than a

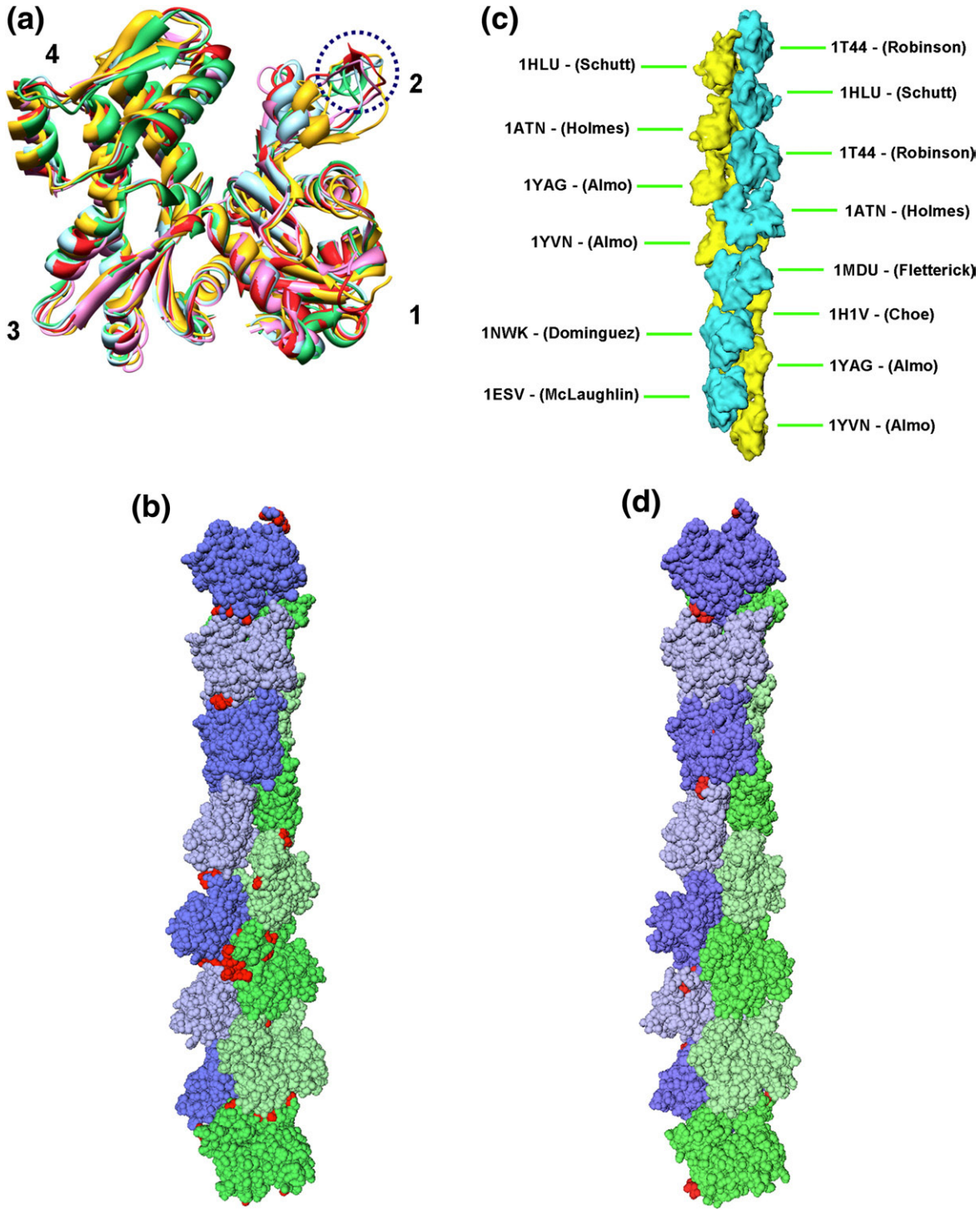

Fig. 1. Actin crystal structure conformations and representation of 14 protomers in the asymmetric unit of the acrosomal actin bundle as a space-filling model. (a) Front view of several representative actin crystal structures illustrating the arrangement of the four actin subdomains and the difference in the secondary structures in subdomain 2, as discussed in the text (and encircled by a blue dashed line here). All the structures were aligned to subdomain 1 of 1ATN. The color scheme is as follows: 1ATN, red; 1HLU, gold; 1J6Z, green; 1YAG, ice blue; and 2BTF, pink. 1HLU (in gold) is obviously in a more open conformation compared with other structures. (b) C_α representation of the asymmetric unit of the acrosomal bundle modeled with Holmes coordinates[5] after energy minimization in the context of the bundle. The actin subunits are shown in a slightly different color and shade. Each amino acid residue is represented by a sphere. Residues colored in red represent those whose C_α moved by more than 2.5 Å from their original coordinates after energy minimization. (c) Protein Data Bank codes and positions of the nine structure coordinate sets (heterogeneous starting model) assigned to the 14 actins in the asymmetric unit. (d) C_α of the heterogeneous starting model for the acrosomal filament after energy minimization.

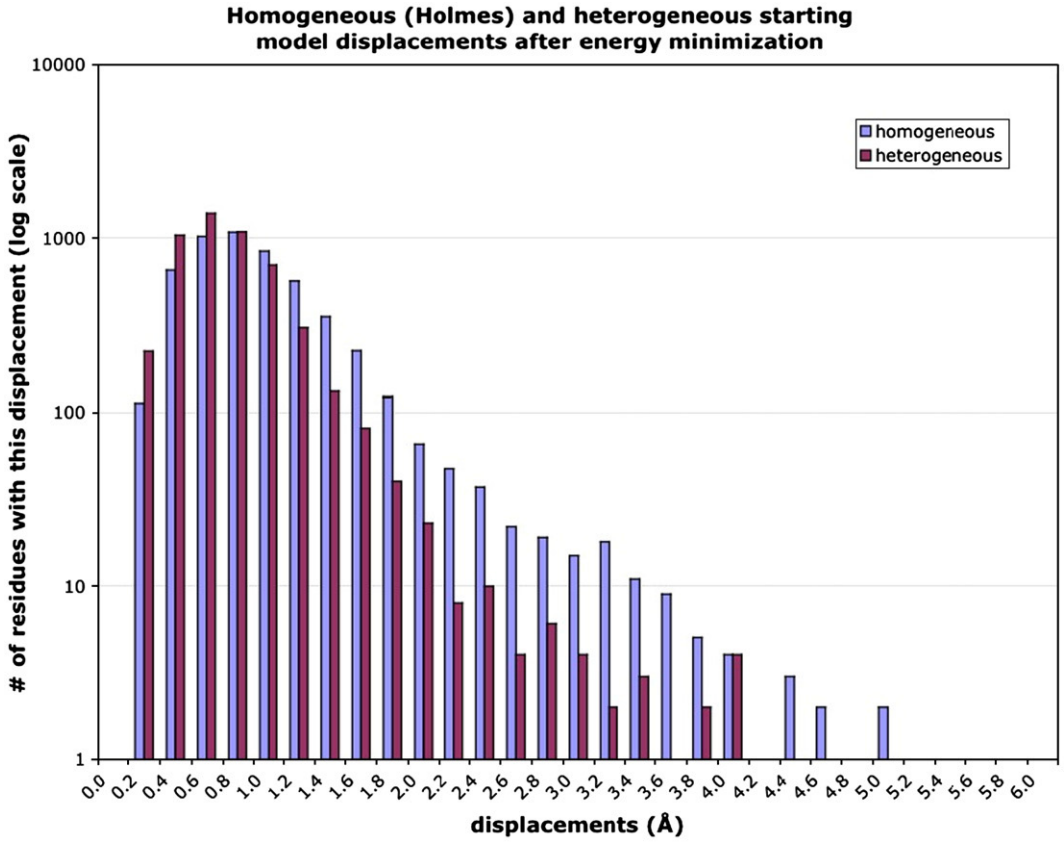

Fig. 2. Histogram of the movement of the C_α coordinates in the acrosomal bundle filament after energy minimization using the homogeneous starting model for every actin subunit *versus* that using the heterogeneous starting model. Coordinates in the *x*-axis are the shift-size bins in angstrom; frequency along the *y*-axis is shown on a log scale to display the wide range of numbers of C_α coordinates in the bins.

single model when fitted to our experimental density. Our cryoEM map is consistent with multiple actin atomic models based on all four conformation groups classified above (and even deviating slightly further from these, as postulated by Klenchin *et al.*,[9] to properly accommodate the acrosomal actin filament), indicating that actin can adopt different conformations when it forms a filament in the acrosomal bundle. This observation is consistent with biochemical evidence revealing that multiple conformations of actin protomers in a filament likely exist at any time.[11] It has been postulated that the hydrophobic plug of actin swings out and inserts into the opposite strand in the filament, stabilizing the filament structure.[5] However, in our heterogeneous model built on multiple actin crystal structures, most of the hydrophobic plugs are not in the extended form. It is noteworthy that recent biochemistry experiments[11,12] support this observation; they demonstrated that rather than being in the extended position, the hydrophobic plug resides predominantly in a "parked" position within the filament but is able to dynamically populate other conformational states. This represents a modification of previous conclusions that favored the hydrophobic plug's extended conformation when it forms a filament.[13] Figure 3 shows the average density map of the 14 actin protomers in the acrosomal bundle asymmetric unit we originally reported.[4] Along with it are the Holmes F-actin model with the extended hydrophobic plug and two representative x-ray coordinate sets of monomeric G-actin. Our density map shows that the average density in this hydrophobic plug region physically lies between the two kinds of conformation for this loop. These biochemical and structural observations support our heterogeneous model.

We earlier established that the twist of the actin filament was affected at the subunit-to-subunit level by the interactions of actin with its binding protein, scruin.[4] We also showed that the orientation of each protomer in the asymmetric unit was unique, again presumably influenced by the environment in the bundle. Our observations here suggest that this influence may even extend to the tertiary structure of the actin subunit because of the better fit of the multiple crystal structures (Fig. 1d). This observation implies that the environment of the actin (i.e., actin–actin, actin–scruin, and scruin–scruin packing interactions in this bundle) has a great influence on the conformation of the individual actin subunits. Such conformational variation has also been observed in G-actin monomer crystals with different co-crystallization partners and crystallization

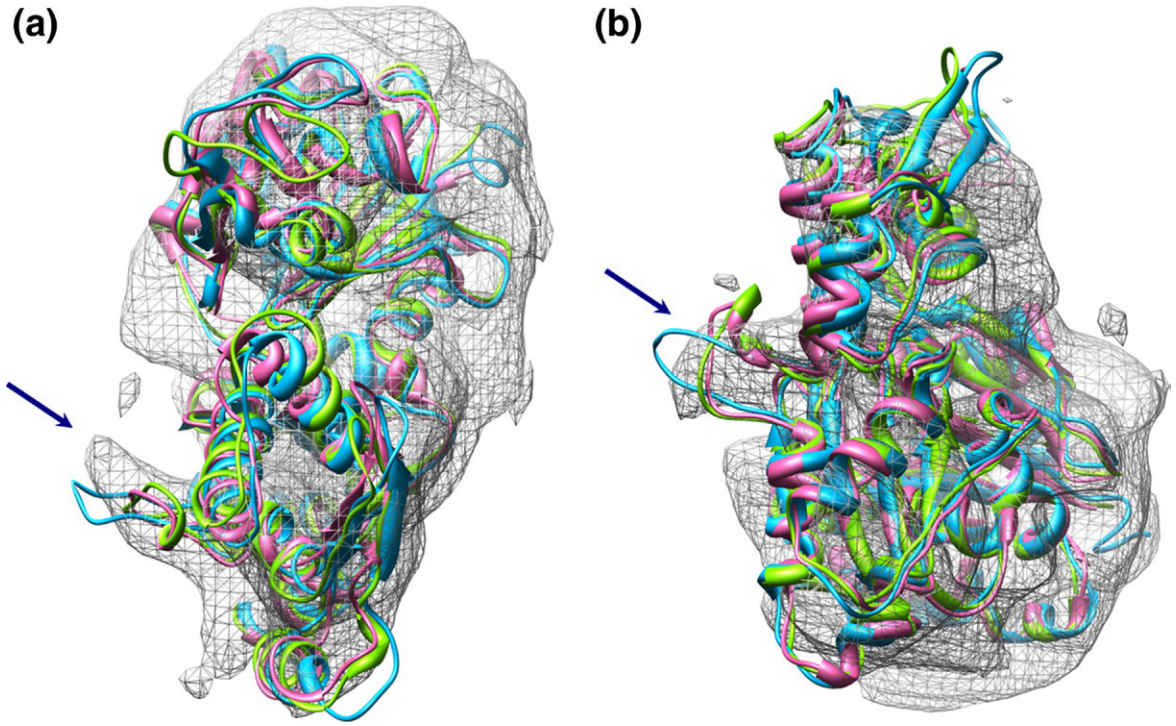

Fig. 3. Average density map of the 14 actin protomers in the acrosomal bundle asymmetric unit[4] along with the Holmes F-actin model (in cyan) and two representative x-ray structures of G-actin monomers (1MDU in light green and 1ESV in pink). Arrows indicate the hydrophobic loop that is extended toward the opposite strand in the Holmes structure and "parked" against its own monomer in the x-ray structures. Our average density is intermediate between these two extremes. (a) Top view, looking approximately down the filament axis. (b) Side view.

conditions.[10] Furthermore, the average twist in F-actin filaments has been seen to vary in the presence of actin-binding proteins[14] or during the process of actin polymerization.[15] All of these studies support the notion that each and every actin protomer in a filament can have different tertiary and quaternary structures depending on its cellular environment. This is further emphasized in Supplemental Figure 1, which shows the variance map based on the 14-protomer average. The variance of the density of subdomains 2, 3, and 4 and the relatively lower variance within subdomain 1 are model-independent measures reinforcing the notion that each of the subdomains in the protomers of the actin filament may adopt a different conformation. In fact, the lower density of subdomains 2 and 4 in our published 14-protomer average map[4] was one of the clues that led us to try different conformers of actin (some of which vary substantially in subdomains 2 and 4) in the first place. The accompanying Protein Data Bank entry is thus the first one for which F-actin density has been used to fit atomic models into a biological filament without the assumption of perfect helical symmetry. It should be noted that these coordinates are different from the original ones for each of these molecules since the energy minimization shifted the coordinates to relieve the steric clashes in the acrosomal filament. Conformational flexibility of actin allows the filament to withstand strain and local distortions and still remain at least partly intact.[11] Since no crystal structure of scruin is available, a full pseudoatomic model of the actin filament with scruin in the context of the acrosomal bundle crystal cannot be established yet. This bundle is a natural system for demonstrating actin structural flexibility without bias because it is both biologically active and experimentally tractable.

Protein Data Bank accession numbers

Coordinates have been deposited with accession codes 3B5U and 3B63.

Acknowledgements

We acknowledge support from the National Institutes of Health (P41RR02250, DK35306, and 2PN2EY016525 through the National Institutes of Health Roadmap for Medical Research) and National Science Foundation (EIA-032645, 1IIS-0705644 and 1IIS-0705474).

Supplementary Data

Supplementary data associated with this article can be found, in the online version at, doi:10.1016/j.jmb.2007.10.027

References

1. Mahadevan, L. & Matsudaira, P. (2000). Motility powered by supramolecular springs and ratchets. *Science*, **288**, 95–100.
2. Shin, J. H., Mahadevan, L., Waller, G. S., Langsetmo, K. & Matsudaira, P. (2003). Stored elastic energy powers the 60-micron extension of the *Limulus polyphemus* sperm actin bundle. *J. Cell Biol.* **162**, 1183–1188.
3. Schmid, M. F., Matsudaira, P., Jeng, T. W., Jakana, J., Towns-Andrews, E., Bordas, J. & Chiu, W. (1991). Crystallographic analysis of acrosomal bundle from *Limulus* sperm. *J. Mol. Biol.* **221**, 711–725.
4. Schmid, M. F., Sherman, M. B., Matsudaira, P. & Chiu, W. (2004). Structure of the acrosomal bundle. *Nature*, **431**, 104–107.
5. Holmes, K. C., Popp, D., Gebhard, W. & Kabsch, W. (1990). Atomic model of the actin filament. *Nature*, **347**, 44–49.
6. Kabsch, W., Mannherz, H. G., Suck, D., Pai, E. F. & Holmes, K. C. (1990). Atomic structure of the actin: DNase I complex. *Nature*, **347**, 37–44.
7. Brunger, A. (1992). X-PLOR (version 3.1): a system for X-ray crystallography and NMR. The Howard Hughes Medical Institute and Department of Molecular Biophysics and Biochemistry, Yale University. http://atb.csb.yale.edu/xplor/.
8. Wriggers, W. & Birmanns, S. (2001). Using Situs for flexible and rigid-body fitting of multiresolution single-molecule data. *J. Struct. Biol.* **133**, 193–202.
9. Klenchin, V. A., Khaitlina, S. Y. & Rayment, I. (2006). Crystal structure of polymerization-competent actin. *J. Mol. Biol.* **362**, 140–150.
10. Sablin, E. P., Dawson, J. F., VanLoock, M. S., Spudich, J. A., Egelman, E. H. & Fletterick, R. J. (2002). How does ATP hydrolysis control actin's associations? *Proc. Natl Acad. Sci. USA*, **99**, 10945–10947.
11. Shvetsov, A., Stamm, J. D., Phillips, M., Warshaviak, D., Altenbach, C., Rubenstein, P. A. *et al.* (2006). Conformational dynamics of loop 262–274 in G- and F-actin. *Biochemistry*, **45**, 6541–6549.
12. Scoville, D., Stamm, J. D., Toledo-Warshaviak, D., Altenbach, C., Phillips, M., Shvetsov, A. *et al.* (2006). Hydrophobic loop dynamics and actin filament stability. *Biochemistry*, **45**, 13576–13584.
13. Shvetsov, A., Musib, R., Phillips, M., Rubenstein, P. A. & Reisler, E. (2002). Locking the hydrophobic loop 262–274 to G-actin surface by a disulfide bridge prevents filament formation. *Biochemistry*, **41**, 10787–10793.
14. McGough, A., Pope, B., Chiu, W. & Weeds, A. (1997). Cofilin changes the twist of F-actin: implications for actin filament dynamics and cellular function. *J. Cell Biol.* **138**, 771–781.
15. Orlova, A., Shvetsov, A., Galkin, V. E., Kudryashov, D. S., Rubenstein, P. A., Egelman, E. H. & Reisler, E. (2004). Actin-destabilizing factors disrupt filaments by means of a time reversal of polymerization. *Proc. Natl Acad. Sci. USA*, **101**, 17664–17668.